A dynamical-statistical forecast model for the annual frequency of western Pacific tropical cyclones based on the NCEP Climate Forecast System version 2

Xun Li,[1] Song Yang,[2] Hui Wang,[3] Xiaolong Jia,[4] and Arun Kumar[3]

Received 13 August 2013; revised 9 October 2013; accepted 21 October 2013; published 14 November 2013.

[1] A dynamical-statistical forecast model for the annual tropical cyclones over the western North Pacific is developed based on the empirical relationship between the actual annual number of tropical cyclones (ANTCs) and the dynamical predictions of large-scale variables by the Climate Forecast System version 2 of the National Centers for Environmental Prediction (NCEP). On interannual time scales, the ANTCs are significantly and negatively correlated with the July–October tropical North Atlantic sea surface temperature, tropical western Pacific vertical zonal wind shear (WPVZWS), and subtropical Pacific geopotential height at 500 hPa (HGT500). They are also positively correlated with the zonal wind at 850 hPa over the tropical Pacific Ocean. Skillful forecasts of the above four potential predictors are made with the 24-member ensemble predictions by the NCEP model. The two-predictor model with the HGT500 and the WPVZWS shows the most skillful hindcasts at 0–2 month leads assessed by the leave-one-out cross validation for the ANTCs over the 31 year record between 1982 and 2012. The corresponding correlation coefficients and the root-mean-square errors (RMSEs) between the observed and hindcast ANTCs are in the ranges from 0.73 to 0.79 and from 3.11 to 2.75, respectively. Observed ANTCs during El Niño–Southern Oscillation events are generally well captured with RMSEs ranging from 3.12 to 3.04 during El Niño years and from 3.62 to 2.44 during La Niña years. The forecast skill of the model for the past 10 years (2003–2012) is competitive with the current forecast schemes. The forecast model initialized in March, May, and June 2013 suggests an inactive season for 2013, with about 22 tropical cyclones.

Citation: Li, X., S. Yang, H. Wang, X. Jia, and A. Kumar (2013), A dynamical-statistical forecast model for the annual frequency of western Pacific tropical cyclones based on the NCEP Climate Forecast System version 2, *J. Geophys. Res. Atmos.*, *118*, 12,061–12,074, doi:10.1002/2013JD020708.

1. Introduction

[2] Reliable prediction of the year-to-year tropical cyclone (TC) activity is of great societal and scientific importance. The variations of TC activity over the western North Pacific (WNP) are primarily due to the El Niño–Southern Oscillation (ENSO) effects by modulating the intensity and location of local monsoon trough and changing the vertical wind shear [e.g., *Camargo and Sobel*, 2005; *Camargo et al*., 2007a; *Chan*, 2000; *Chen et al*., 1998; *Wu et al*., 2012]. During an El Niño event, TCs tend to form over the southeastern WNP and can develop very intensively [*Chan*, 2000; *Wang and Chan*, 2002; *Camargo and Sobel*, 2005; *Chan*, 2007; *Camargo et al*., 2007a, 2007b]. Moreover, the central Pacific El Niño (also known as El Niño Modoki) events [*Ashok et al*., 2007] are shown to shift the TC formation westward to the western Pacific [*Kim et al*., 2010]. In addition, the variations of TC frequency are also related to other factors, for example, the quasi-biennial oscillation in the stratosphere [*Chan*, 1995; *Ho et al*., 2009], winter or spring sea ice cover over the North Pacific [*Fan*, 2007a], the North Pacific oscillation [*Wang and Fan*, 2007], the Antarctic Oscillation [*Wang et al*., 2007], Hadley circulation and the sea surface temperature (SST) near Australia [*Zhou and Cui*, 2008; *Zhou and Cui*, 2011], and the boreal summer SST anomalies in the eastern Indian Ocean [*Zhan et al*., 2011].

[3] Following the pioneering work of statistical forecasts for seasonal Atlantic hurricane activity [*Gray*, 1984a, 1984b], various seasonal forecasting techniques have been applied to issue forecasts for TCs over the Atlantic basin and other basins. Several statistical seasonal prediction schemes using the empirical relationships between target

[1]Hainan Meteorological Service, China Meteorological Administration, Haikou, China.
[2]School of Environmental Science and Engineering, Sun Yat-sen University, Guangzhou, China.
[3]NOAA/NWS/NCEP Climate Prediction Center, Camp Springs, Maryland, USA.
[4]National Climate Center, China Meteorological Administration, Beijing, China.

Corresponding author: S. Yang, School of Environmental Science and Engineering, Sun Yat-sen University, 135 W. Xingang Rd., Haizhu District, Guangzhou 510275, China. (yangsong3@mail.sysu.edu.cn)

2169-897X/13/10.1002/2013JD020708

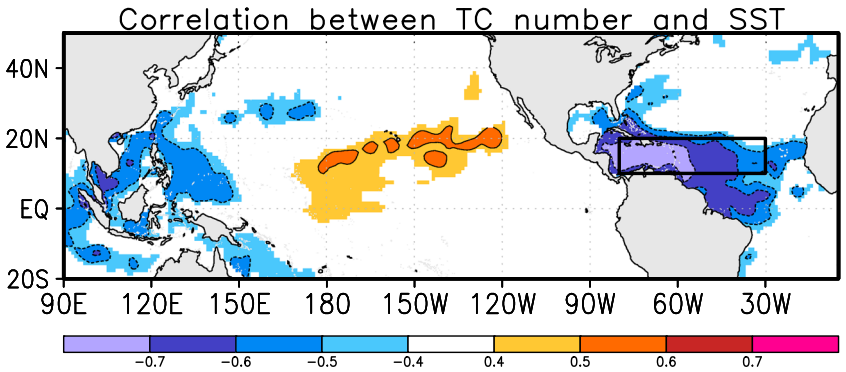

Figure 1. Spatial map of correlations between observed annual number of tropical cyclones (ANTCs) over western North Pacific and June–October (JASO) mean sea surface temperature (SST) from observation for the period 1982–2012. The bold box identifies the primary regions for predictor selection (see Table 1).

season TC activity and influential preceding large-scale variables have been developed and applied to operational prediction [e.g., *Gray et al*., 1993, 1994; *Elsner and Schmertmann*, 1993; *Klotzbach and Gray*, 2004; *Chu and Zhao*, 2007]. For the WNP basin, real-time forecasts of the annual number of TCs (ANTCs) were first undertaken as an operational scheme that included predictors from the environment conditions and factors related to ENSO around 2000 [*Chan et al*., 1998, 2001], and an updated version was established later [*Chan*, 2008]. Recently, new statistical schemes based on both local and remote influences were developed for predicting the frequency of intense TCs over WNP [*Fan*, 2007b; *Fan and Wang*, 2009]. Most of these statistical forecasts are first issued before or at the beginning of TC season and then updated in the early part of the season.

[4] In addition to the purely statistical approaches, state-of-the-art dynamic models are used to perform seasonal prediction of TC activity in the recent years. In the last decade, the skill of dynamic model-based approaches for predicting the seasonal TC activity over the North Atlantic and the eastern Pacific is comparable to that of statistical schemes [*Vitart*, 2006; *Vitart et al*., 2007; *Zhao et al*., 2010; *Chen and Lin*, 2011]. The direct dynamical approach, however, is rather unreliable in predicting the TC activity over the WNP basin, due likely to lack of strong correlation between TC activity and local SST [*Chen and Lin*, 2013]. The dynamical-statistical approach that provides an alternative way to predict seasonal TC activity has been developed in the recent years. Based on the statistical relationships between the interannual variability of TC frequency and the physically relevant concurrent or future large-scale conditions from ensemble forecasts of dynamical models, the so-called hybrid dynamical-statistical models for predicting the seasonal TC activity over the Atlantic and WNP basins have been established [*Wang et al*., 2009; *Kim and Webster*, 2010; *Vecchi et al*., 2011; *Sun and Chen*, 2011; *H.-S. Kim et al*., 2012]. Encouragingly, these hybrid models have displayed significant skills in predicting TC activity.

[5] In this study, a hybrid model for predicting the annual TC activity over the WNP is developed using the combination of the National Centers for Environmental Prediction (NCEP) Climate Forecast System version 2 (CFSv2) and an empirical linear regression model. The CFSv2 is a fully coupled ocean-land-atmosphere dynamical model that represents a significant modification to model components, data assimilation system, and ensemble configuration and provides operational seasonal predictions at NCEP (S. Saha et al., The NCEP Climate Forecast System version 2, submitted to *Journal of Climate*, 2013). Previous studies have suggested that the model can skillfully capture ENSO and its related features over the tropics and the North Pacific [*H.-M. Kim et al*., 2012a, 2012b] and the air-sea interaction in the North Atlantic [*Hu et al*., 2012]. It has also been demonstrated that the model is capable of capturing and predicting many features of the Asian monsoon [e.g., *Jia and Yang*, 2013; *Jiang et al*., 2013a, 2013b; *Liu et al*., 2013]. Incorporating with the predictors provided by the skillful CFSv2 seasonal forecasts, we here show that the hybrid-type model makes significant advances on current statistical schemes used for the WNP basin [e.g., *Chan et al*., 2001].

[6] The rest of this study is organized as follows. Section 2 introduces the details of forecast and observational data and the prediction techniques applied. Section 3 presents the observational relationships between the interannual variability of WNP TCs and oceanic/atmospheric variables. The CFSv2 predictive skills for large-scale variables are described in section 4. Section 5 presents results from the hybrid model for predicting the WNP TC activity. Finally, concluding remarks are given in section 6.

2. Data and Methods

[7] The present study takes advantage of the observational data that include the TC best track data set for the WNP, the monthly mean SSTs, and the monthly mean atmospheric fields for 1982–2012. The actual ANTCs over the WNP, representing TC activity, are from the Regional Specialized

Table 1. List of Regions for Defining Predictors and 4-Month (JASO) Averaged Correlation (COR) Between the Observed Predictors and ANTC Series[a]

Predictors	Latitude	Longitude	COR
NATLSST	10–20°N	280°W–330°W	−0.72
WPVZWS	10–20°N	130°E–190°W	−0.73
U850	10–20°N	130°E–190°W	0.67
HGT500	10–30°N	120°E–160°E	−0.69

[a]All correlations significantly exceed the 99% confidence level estimated by the Monte Carlo test.

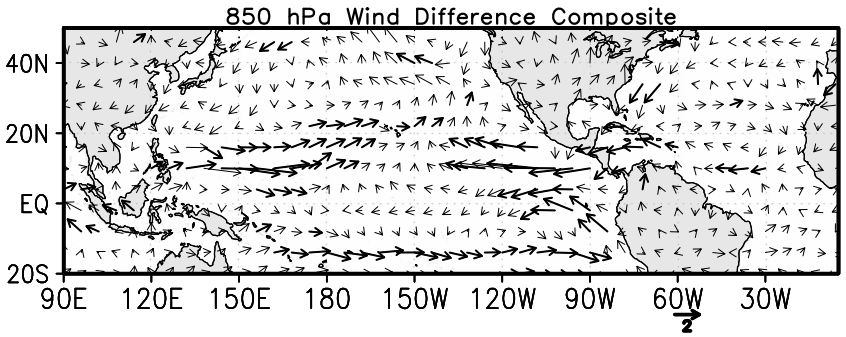

Figure 2. Observed composite differences between active TC years and inactive TC years for 850 hPa wind (vector, m s^{-1}). Thick arrows indicate areas where the difference in wind speed is larger than 1.0 m s^{-1}

Meteorological Center Tokyo–Typhoon Center best track data set. Here we only use the TCs with maximum sustained wind speed reaching or exceeding 34 kt (17.0 m s^{-1}).

[8] The observational SSTs are taken from the National Oceanic and Atmospheric Administration (NOAA) optimum interpolation SST version 2 (OISST v2) [*Reynolds et al.*, 2002]. The observational atmospheric fields, including the zonal winds at 200 hPa and 850 hPa and the geopotential height at 500 hPa, are from the NCEP CFS Reanalysis (CFSR) [*Saha et al.*, 2010]. The vertical zonal wind shear (VZWS) is defined as the difference between the 200 hPa and 850 hPa zonal winds.

[9] The CFSv2 9 month retrospective forecast (or hindcast) data set covers a 29 year period from 1982 to 2010 (Saha et al., submitted manuscript, 2013). The ensemble hindcasts run every 5 days from the 00, 06, 12, and 18 UTC cycles over that period. The CFSv2 data for years 2011 and 2012 are taken from the CFSv2 9 month real-time products, which have been implemented operationally at the NCEP since 2011. Details about the CFSv2 and the data are given by Saha et al. (submitted manuscript, 2013).

[10] About 75% of the WNP TCs are formed during July, August, September, and October (JASO), the main TC season. Thus, our analysis focuses on the statistical relationship between the interannual variability of WNP TCs and the oceanic and atmospheric conditions in JASO. In the CFSv2, we use 24-member ensemble seasonal forecasts for target season JASO with 24 different initial conditions (ICs) in each month from January to June, which correspond to the forecasts of 5, 4, 3, 2, 1, and 0 month leads, respectively.

[11] All seasonal mean observational and CFSv2-predicted oceanic and atmospheric data are derived by averaging the monthly mean values over JASO with a horizontal resolution of 1° × 1° (latitude and longitude). To identify the potential predictors for ANTCs, we examine the simultaneous correlations between the ANTC time series and large-scale environments from observations and CFSv2 forecasts, respectively. The CFSv2 forecast skill for a target season is calculated as an anomaly correlation based on the ensemble mean of seasonal predictions and the JASO observations. The JASO season anomalies of all variables are determined based on the 31 year climatology of 1982–2012. The statistical significance of the correlations is estimated by the Monte Carlo technique outlined by *Wilks* [2006].

[12] For the hybrid dynamical-statistical model for ANTC predictions, we employ the empirical prediction system highlighted by *Wang et al.* [2009]. The system is known as a simple linear (one predictor only) or multiple linear (multiple predictors) regression analysis between the area-averaged CFSv2 forecasts of JASO anomalies and the ANTC time series over the 31 year period.

[13] To assess the hybrid model forecast skill, a leave-one-out cross-validation method is applied. In this approach, the model is trained for all ANTCs years except for one target year and a hindcast is made for that year. Using the hindcasts in the leave-one-out cross-validation method, the mean square skill scores

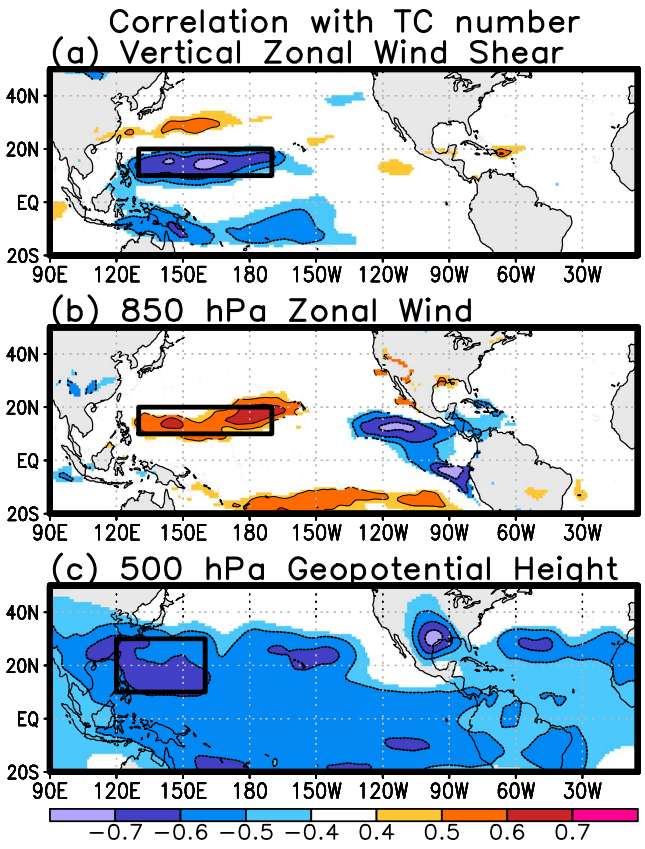

Figure 3. Same as Figure 1 but for (a) vertical zonal wind shear (200 hPa–850 hPa), (b) zonal wind at 850 hPa, and (c) geopotential height at 500 hPa from observations for the period 1982–2012. The bold boxes identify the primary regions for predictor selection (see Table 1).

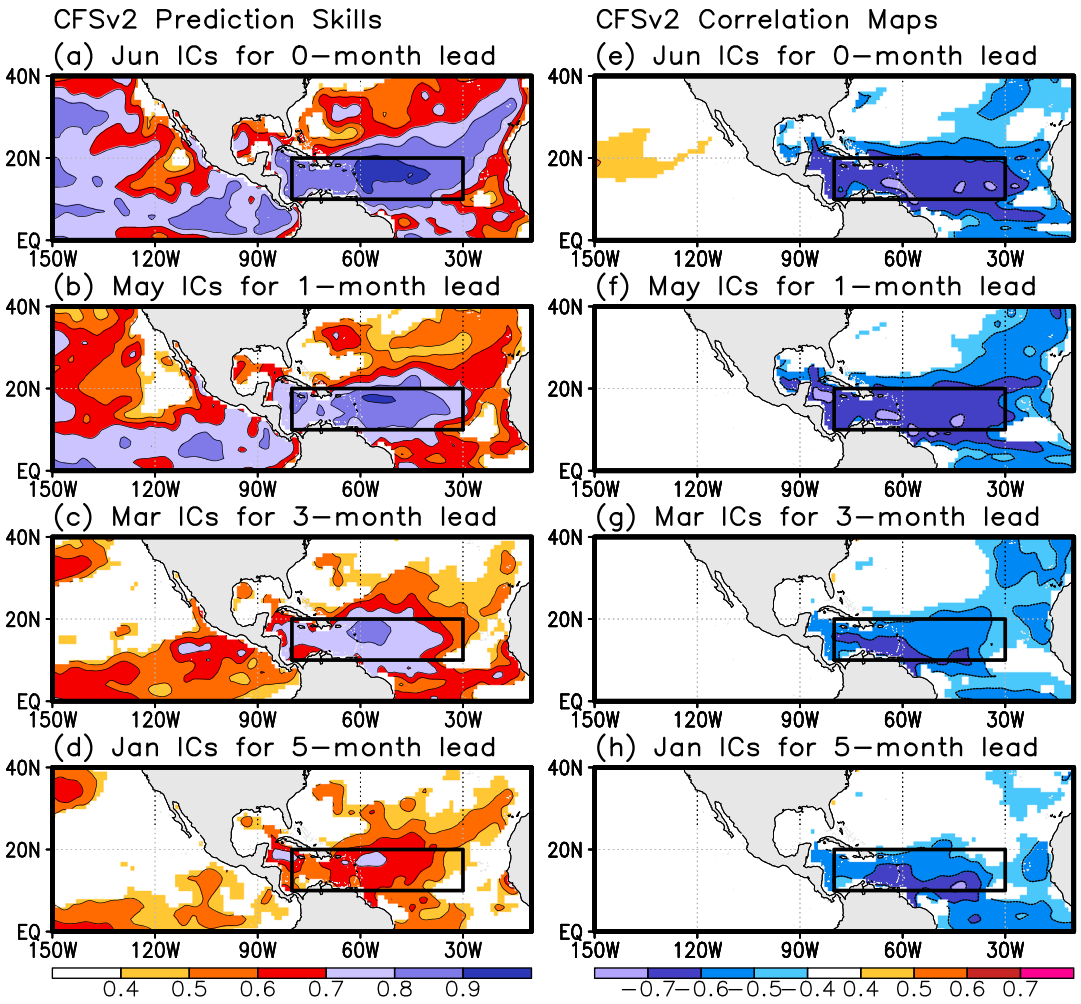

Figure 4. Anomaly correlation maps between (left column) observed and CFSv2-predicted JASO SSTs and (right column) CFSv2-predicted JASO SSTs with the time series of ANTCs from 1982 to 2012. The CFSv2-predicted JASO SSTs are 24-member ensemble mean forecast with (a, e) June, (b, f) May, (c, g) March, and (d, h) January initial conditions. Shadings indicate the correlations exceeding the 95% confidence level (Monte Carlo test). The bold boxes are the same as in Figure 1.

(MSSSs) are calculated from the mean square error (MSE), as expressed by *H.-S. Kim et al.* [2012]:

$$\mathrm{MSSS} = 1 - \frac{\mathrm{MSE}_{\mathrm{model}}}{\mathrm{MSE}_{\mathrm{obs}}} = 1 - \frac{\frac{1}{n}\sum_{i=1}^{n}\left(f_i^{\mathrm{obs}} - f_i\right)^2}{\frac{1}{n}\sum_{i=1}^{n}\left(f_i^{\mathrm{obs}} - f^{\mathrm{obs}}\right)^2}, \qquad (1)$$

where n is the total number of years, f_i^{obs} and f_i are the numbers of WNP TCs from observation and hindcast for the ith year, respectively, and f^{obs} is the observational mean number of WNP TCs. The MSSS is a metric for the skill comparison of the present model and climatology-based forecasts, with high values indicating a good model.

3. Potential Predictor Identification

[14] To identify the potential ANTC predictors, we select predictor variables on the basis of coefficients of spatial correlation between the ANTCs and large-scale environment from observations and CFSv2 forecasts. Previous studies have indicated that candidate variables for potential predictors are mostly limited to SSTs, VZWS, 850 hPa zonal wind, and 500 hPa geopotential height [e.g., *Chan et al.*, 2001; *Wang et al.*, 2009; *Werner and Holbrook*, 2011].

[15] Figure 1 shows the spatial map of the correlations between ANTC time series and observed SST for the JASO season. Positive correlations prevail over the tropical central Pacific, while significant negative correlations exist over the tropical North Atlantic, implying that the interannual variations of WNP TCs are not only linked to the central Pacific El Niño [*H.-M. Kim et al.*, 2011; *Richard et al.*, 2012] but also strongly and negatively correlated with the tropical North Atlantic SSTs. It has been suggested previously that the positive SST anomalies of the tropical North Atlantic are mainly due to the Pacific ENSO teleconnection at both interannual and decadal time scales [e.g., *Enfield and Mayer*, 1997; *Chang et al.*, 1997; *Huang et al.*, 2002; *Liu et al.*, 2004; *Hu et al.*, 2011]. More importantly, the tropical North Atlantic SST forcing is the main cause of the WNP anomalous anticyclones associated with reduced convections [*Lu and Dong*, 2005; *Rong et al.*, 2010]. Thus, the interannual variations of

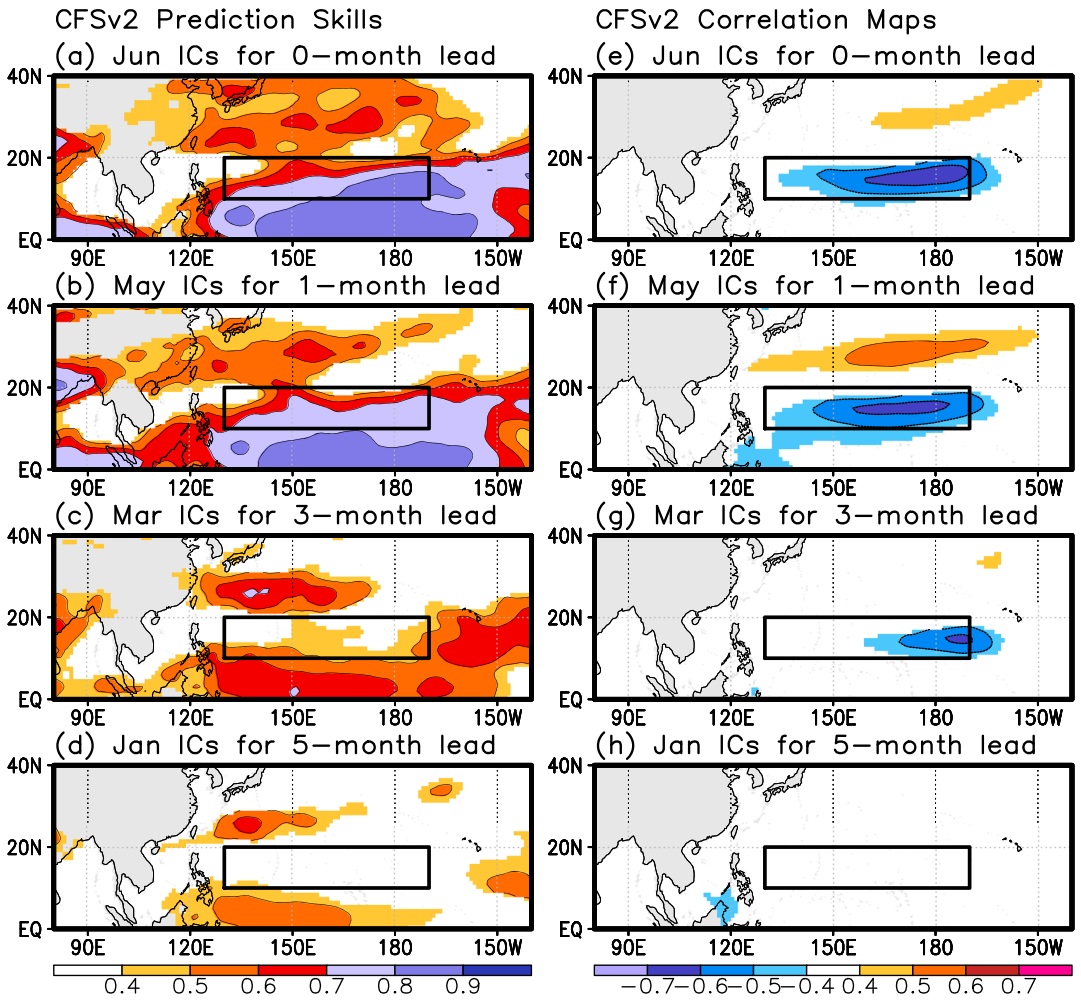

Figure 5. Same as Figure 4 but for CFSv2-predicted JASO VZWS. The bold boxes are the same as in Figure 3a.

WNP TCs are likely resulted from the changes in the planetary-scale atmospheric circulation associated with ENSO [*Chan*, 2007], which is consistent with the previous finding that there is no strong local correlation between the SST anomalies and TC activity over the WNP [e.g., *Wang and Chan*, 2002; *Chan and Liu*, 2004]. Therefore, we derive a tropical North Atlantic SST (NATLSST) index as a potential predictor (see Table 1) by averaging the JASO mean SST over the tropical North Atlantic (10–20°N, 280–330°W), a region with significant negative correlations (Figure 1).

[16] Figure 2 illustrates the composite differences in observed 850 hPa winds between active WNP TCs years (ANTCs ≥ 29) and inactive years (ANTCs ≤ 22). Here we identify 1986, 1988, 1989, 1990, 1991, 1992, 1994, and 2004 (1998, 1999, 2003, 2008, 2009, 2010, and 2011) as the active (inactive) TC years, which represent about 26% (23%) of the total number of years in the period of investigation. The remaining years are considered neutral. The anomalies of 850 hPa winds indicate that an eastward extension of the monsoon trough coincides with reduced VZWS, which implies a favorable large-scale environmental factor for TC formation [*Zhao et al.*, 2011; *Wu et al.*, 2012]. In contrast, the anomalous anticyclone over the central Pacific and WNP, due mainly to the tropical North Atlantic warming [*Lu and Dong*, 2005; *Rong et al.*, 2010], is related to the TC inactivity.

[17] As shown in Figure 3, which displays the spatial correlations between the ANTC series and the observed atmospheric variables for JASO season, the correlation patterns for VZWS and 850 hPa zonal wind (Figures 3a and 3b) are consistent with the 850 hPa wind anomaly map (Figure 2). The VZWS and 850 hPa zonal wind correlation patterns over the tropical WNP, the main development region for WNP TCs, reflect that reduced (increased) VZWS and eastward extension (westward retreat) of the monsoon trough are favorable (unfavorable) for TC genesis. The 500 hPa geopotential height exhibits strong negative correlation throughout the tropical and subtropical Pacific, maximizing in the WNP, whereby colder middle-lower troposphere air masses support the development of TCs (Figure 3c). The regions with significant correlations, indicated by the boxes in Figure 3, are used to construct circulation indices as the potential predictors for ANTCs.

[18] According to the patterns of correlations between ANTCs and the circulation fields, four candidate indices, namely, WPVZWS, U850, HGT500, and NATLSST, are used as potential ANTC predictors (see boxes in Figures 1 and 3). The definitions of each predictor index and their

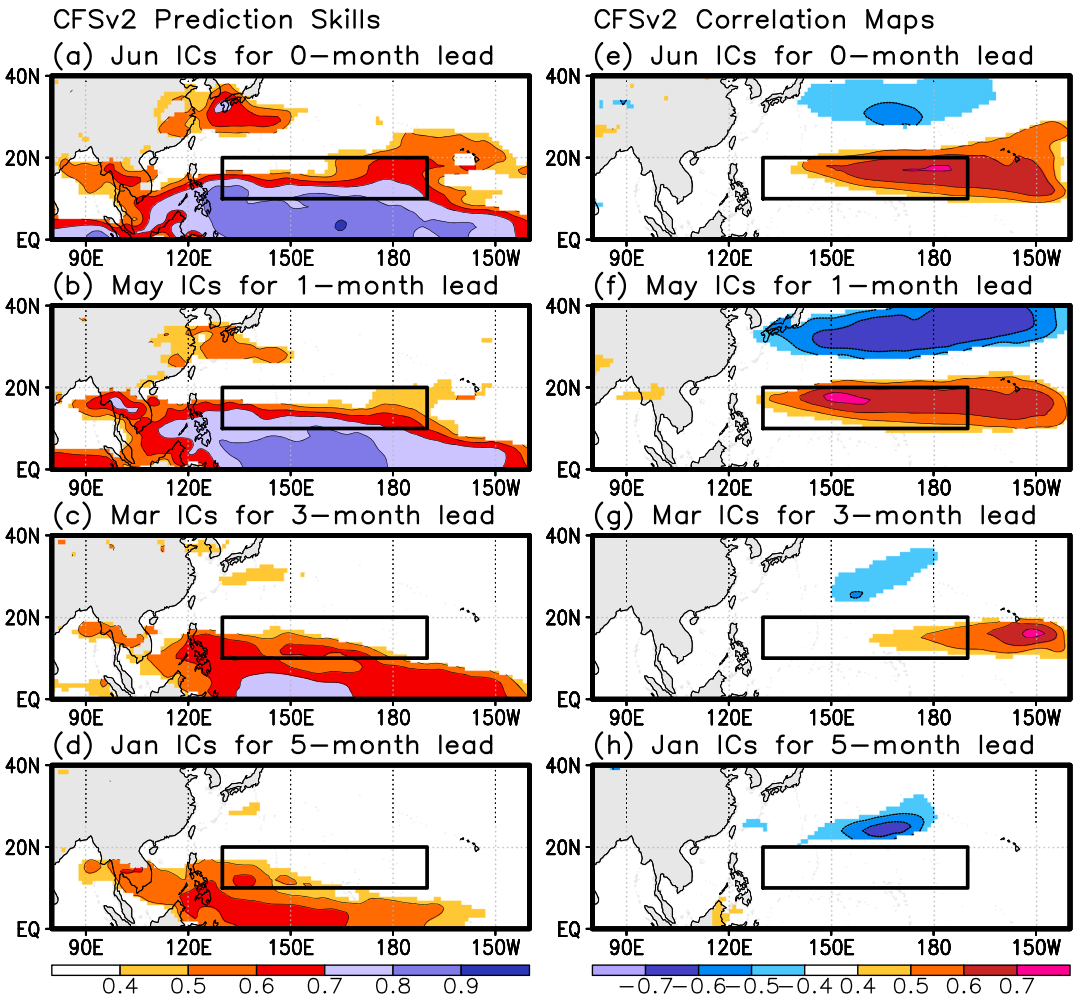

Figure 6. Same as Figure 4 but for CFSv2-predicted JASO U850. The bold boxes are the same as in Figure 3b.

correlations with ANTCs are listed in Table 1. All correlation coefficients exceed the 99% confidence level estimated by the Monte Carlo test. The correlation coefficients for ANTCs with the NATLSST and WPVZWS indices are over −0.72.

4. CFSv2 Prediction Skills

[19] The CFSv2 prediction skills for the atmospheric and oceanic variables and the correlations between ANTCs and the CFSv2-predicted SST/atmospheric fields over selected regions are examined here. Figure 4 (left column) presents the simultaneous correlation between the observations and the CFSv2-predicted ensemble mean JASO SST from 5 to 0 month leads. In general, the CFSv2 has a significant skill in forecasting JASO SST in the tropical North Atlantic, the ANTC oceanic predictor region. As expected, the predictive skill is higher in shorter time leads. The maximum correlations are above 0.9 at the 0 month and 1 month leads (Figures 4a and 4b) and around 0.7 at the 3 month lead (Figure 4c). The maximum correlations are below 0.7 in the 4 month (not shown) and 5 month predictions (Figure 4d). The spatial maps of correlation between ANTCs and CFSv2 forecasts of JASO SST are also shown in Figure 4 (right column), with similar features found in the observations (Figure 1). The shorter is the lead time, the more significant are the negative correlations in the western North Atlantic between 10°N and 20°N (Figures 4e–4h).

[20] Figure 5 (left column) shows the correlations between the observations and the CFSv2-predicted ensemble mean JASO VZWS from 5 month to 0 month leads. Significant skill is found over the western tropical Pacific. The anomaly correlation is as high as 0.8 at the 0–1 month leads (Figures 5a and 5b). The skill decreases over the western Pacific with increase in forecast lead time. The correlation is 0.4 at the 3 month lead (Figure 5c) and less significant at the 4 and 5 month leads (Figure 5d). The significant negative correlations between VZWS and ANTCs in the western subtropical Pacific in observations are also found in the forecast with June (Figure 5e), May (Figure 5f), and April (not shown) ICs but not with March (Figure 5g), February (not shown), and January (Figure 5h) ICs. Similar results are found in the CFSv2 forecasts for U850 (Figure 6).

[21] Figure 7 (left column) displays the correlations between observations and CFSv2-predicted ensemble mean JASO 500 hPa geopotential height from 5 month to 0 month leads. Significant skill is found over the western tropical Pacific, while the skill is relatively low in the predictor area. The

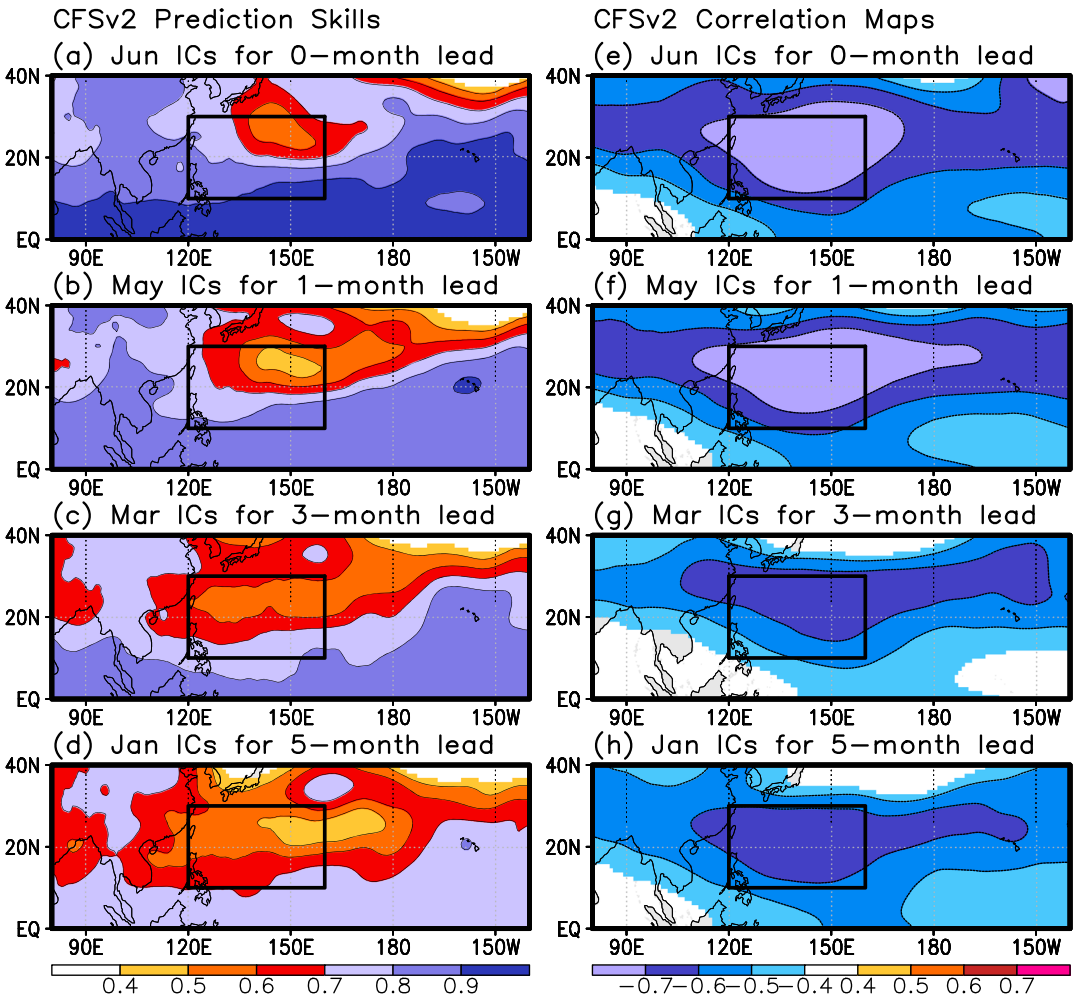

Figure 7. Same as Figure 4 but for CFSv2-predicted JASO HGT500. The bold boxes are the same as in Figure 3c.

anomaly correlation is as high as 0.7 at the 0–1 month leads (Figures 7a and 7b). As compared to VZWS and 850 hPa zonal wind in the predictor regions (Figures 5 and 6), the predictive skill for 500 hPa geopotential height in the predictor regions is less sensitive to forecast lead time, and the skill at the 3 and 5 month leads (Figures 7c and 7d) is only slightly lower than that at the 0–1 month leads (Figures 7a and 7b). The negative correlations with ANTCs in the western subtropical Pacific in observations are found in the forecasts with June–January ICs (right column). The correlations at the shorter leads (Figures 7e and 7f) are even slightly more significant than those in observations (Figure 3c).

[22] Figure 8 presents the forecast skill for the four potential predictors for all 24 individual ensemble members. In general, the correlations between the ensemble mean forecast and observations are much higher than those of individual members, particularly for WPVZWS and U850. For NATLSST, the forecast skills for individual members (Figure 8a, gray curves) are close to those of ensemble mean (Figure 8a, black curve) for 0–2 month leads. Beyond 2 months, the individual member forecast skills are substantially lower than the ensemble mean skill. For WPVZWS and U850 (Figures 8b and 8c), correlations vary greatly and forecast uncertainty increases significantly in the long leads. For HGT500, however, the correlations and spreads of individual member skills are less sensitive to forecast lead time (Figure 8d). Overall, individual correlations are weaker than those of ensemble mean CFSv2 forecasts. It is therefore expected that the predictors derived from the ensemble mean forecasts are more effective than those from the individual members for the ANTC forecast.

[23] Due to the changes in satellite observations in 1999 that are assimilated in the CFSR [*Xue et al.*, 2011; *Wang et al.*, 2011], the CFSv2 prediction skills for individual variables are also examined using two sets of climatologies (1982–1998 and 1999–2012). Results show that the CFSv2 provides slightly lower skill for predictor NATLSST and HGT500, and slightly higher skill for WPVZWS and U850 (not shown), suggesting that using the 1982–2012 climatology should not limit the hybrid system capability.

5. Empirical Prediction for TC Activity With CFSv2

5.1. Model Validation

[24] We now employ a simple linear (one predictor only) and multiple linear (multiple predictors) regression analysis between the area-averaged CFSv2 forecast anomalies for

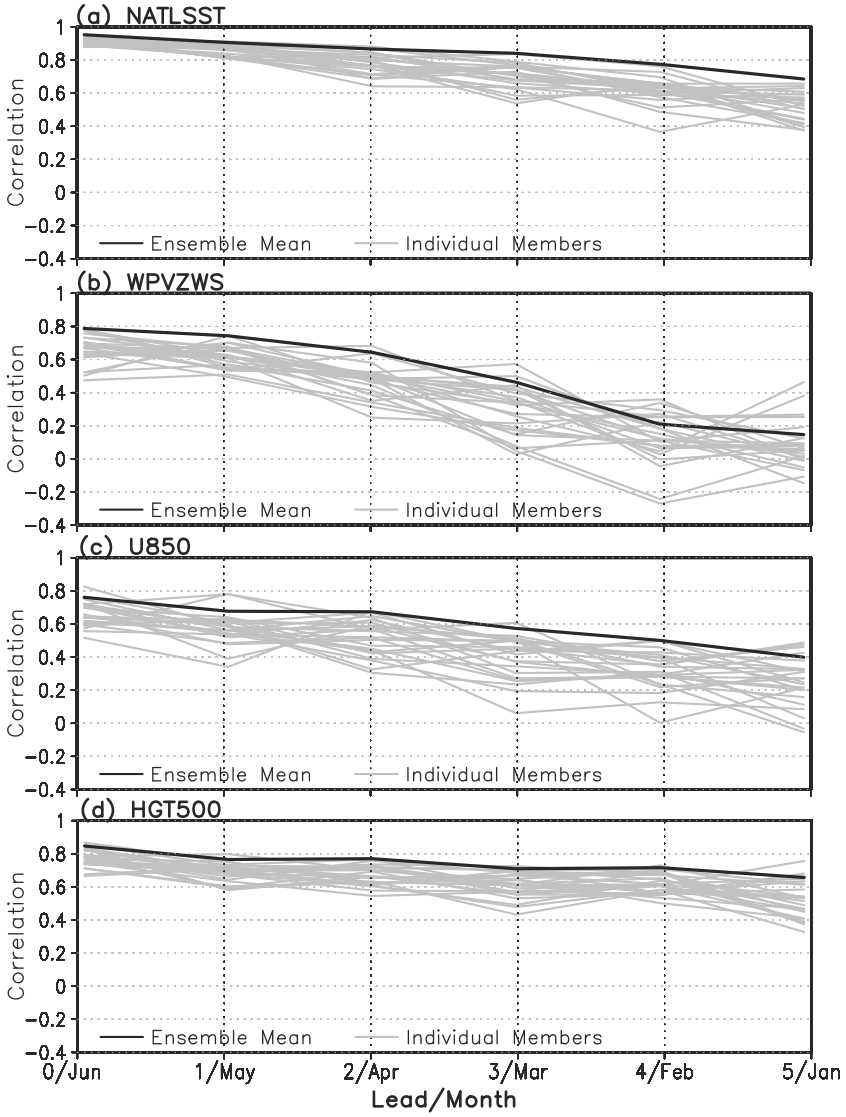

Figure 8. Temporal correlations between observed and CFSv2-predicted (a) NATLSST, (b) WPVZWS, (c) U850, and (d) HGT500 with time leads from 0 month to 5 months. Gray curves are for 24 individual members and black ones are for 24-member ensemble means.

JASO and the observed interannual variations of ANTCs over the 31 year period. Table 2 shows the hindcast skills of ANTCs for 1982–2012 based on four individual potential predictors from the June to January ICs. In general, the best single predictor is HGT500, with correlations and root-mean-square errors (RMSEs) between the observation and the forecast around 0.7 and 3.2, while the predictor with the least utility as a single predictor is U850, with correlations and RMSEs around 0.4 and 4.1 from 0 to 2 month leads. Meanwhile, using HGT500, the MSSSs are above 0.5, indicating a skill improvement of at least 50% for the model over the climatology-based forecasts. The hindcasts also capture the variability in the observed number of TCs within one standard deviation of the 24-member spreads, with about 60% success rate (SRATE) of the ANTC hindcasts for the April–June ICs. The MSSSs and SRATEs for the U850 are around 0.2 and 60%, respectively. The SRATEs of the U850 are comparable to those of HGT500 due mainly to the spread of U850 forecast is larger. For NATLSST and HGT500, the prediction skills of the hindcasts decrease from 3 month to 5 month leads with the correlations, RMSEs, MSSSs, and SRATEs around 0.5, 3.8, 0.3, and 50%, respectively. In contrast, the forecast skills using WPVZWS and U850 singularly decrease significantly because of the poor CFSv2 forecast skill for these two predictors in the long leads, with the correlations, RMSEs, MSSSs, and SRATEs around 0.1, 4.7, −0.1, and 40%, respectively.

[25] We next perform the hindcast of the interannual variability of WNP TCs by combining potential predictors. Owing to the substantial influence of ENSO, it is not easy to obtain the predictors that are entirely and physically independent of each other [*H.-S. Kim et al*., 2012]. Table 3 presents a correlation matrix for the four potential predictors at different time leads. The correlation between NATLSST and HGT500 in observations is 0.78. The remote SST may exert an influence on the WNP TC activity by altering the large-scale circulation over WNP, which is consistent with the previous

Table 2. Model Skills for One-Predictor NATLSST, WPVZWS, U850, and HGT500 From January To June Initial Conditions[a]

Initial Conditions	COR	RMSE	MSSS	SRATE (%)
		NATLSST		
Jun	0.65	3.43	0.42	52
May	0.67	3.35	0.45	42
Apr	0.62	3.55	0.38	48
Mar	0.56	3.74	0.31	55
Feb	0.54	3.82	0.28	55
Jan	0.51	3.93	0.24	58
		WPVZWS		
Jun	0.59	3.64	0.35	65
May	0.52	3.86	0.26	55
Apr	0.62	3.54	0.38	65
Mar	0.33	4.30	0.09	55
Feb	−0.11	4.72	−0.10	42
Jan	0.00	4.70	−0.09	48
		U850		
Jun	0.41	4.16	0.15	55
May	0.48	3.97	0.22	65
Apr	0.41	4.14	0.16	55
Mar	0.15	4.55	−0.02	39
Feb	0.07	4.61	−0.05	45
Jan	−0.01	4.70	−0.09	42
		HGT500		
Jun	0.71	3.17	0.50	58
May	0.73	3.10	0.52	58
Apr	0.71	3.16	0.51	61
Mar	0.54	3.80	0.29	45
Feb	0.50	3.91	0.25	42
Jan	0.58	3.70	0.33	48

[a]Shown are the correlation coefficients (COR), the root-mean-square errors (RMSEs), and the mean square skill scores (MSSSs) between observed and hindcast ANTCs that validate the skill of the model. Success rate (SRATE) is for capturing the variability in ANTCs within hindcast boundaries of standard deviation.

finding that the tropical North Atlantic SST anomalies are positively correlated with the WNP anomalous anticyclone [*Lu and Dong*, 2005; *Rong et al*., 2010]. Meanwhile, the correlations between other combinations of predictors in observations are weaker than ±0.75. The correlations between NATLSST and HGT500, as well as between WPVZWS and U850, in the CFSv2 of all forecast leads are around ±0.9, stronger than those in observations. These two-predictor combinations are excluded in further analysis due to collinearity [*Werner and Holbrook*, 2011]. The links of rest combinations of two predictors in the CFSv2 predictions are weaker than those in observations. Furthermore, the CFSv2-predicted predictor combinations with correlations weaker than ±0.8 are investigated.

[26] Table 4 shows the hindcast skills of ANTCs for 1982–2012 based on two predictors from the CFSv2 June to January ICs. Overall, the two-predictor combinations, NATLSST + WPVZWS, HGT500+ WPVZWS, and HGT500 + U850, provide further reductions of RMSEs than those of the best single predictor HGT500 at most time leads except for NATLSST + U850.

[27] For the NATLSST and WPVZWS combination, the correlation is moderately high, around 0.74, and the RMSE ranges from 3.04 to 3.09 at the 0–2 month leads (Table 4). The MSSS is above 0.53, showing a skill improvement of at least 50% for the model over the climatology-based forecasts. The hindcasts capture the variability in the observed number of TCs within the one standard deviation of the 24-member spreads, with a 58% SRATE of the ANTC hindcasts at the 0 and 1 month leads and above 70% SRATE of the ANTC hindcasts at the 2 and 3 month leads. For the longer leads, the hindcasts exhibit relatively low skill. With increased leads, the correlations, RMSEs, MSSSs, and SRATEs vary from 0.61 to 0.46, 3.59 to 4.08, 0.37 to 0.18, and 71% to 55%, respectively.

Table 3. Correlation Matrix Among the Four Predictors From Both Observations and CFSv2 Ensemble Forecasts, and the ANTC Series

Predictor	HGT500	U850	WPVZWS
	NATLSST		
Observations	0.78	−0.47	0.75
0 month lead with Jun ICs	0.92	−0.47	0.55
1 month lead with May ICs	0.94	−0.46	0.48
2 month lead with Apr ICs	0.93	−0.35	0.50
3 month lead with Mar ICs	0.95	−0.22	0.33
4 month lead with Feb ICs	0.94	−0.38	0.31
5 month lead with Jan ICs	0.88	−0.49	0.54
	WPVZWS		
Observations	0.59	−0.75	1.0
0 month lead with Jun ICs	0.53	−0.87	1.0
1 month lead with May ICs	0.46	−0.91	1.0
2 month lead with Apr ICs	0.52	−0.92	1.0
3 month lead with Mar ICs	0.32	−0.91	1.0
4 month lead with Feb ICs	0.22	−0.92	1.0
5 month lead with Jan ICs	0.29	−0.96	1.0
	U850		
Observations	−0.58	1.0	
0 month lead with Jun ICs	−0.46	1.0	
1 month lead with May ICs	−0.45	1.0	
2 month lead with Apr ICs	−0.35	1.0	
3 month lead with Mar ICs	−0.16	1.0	
4 month lead with Feb ICs	−0.27	1.0	
5 month lead with Jan ICs	−0.25	1.0	

Table 4. Same as Table 2 But for Selected Predictors NATLSST and WPVZWS, NATLSST and U850, HGT500 and WPVZWS, and HGT500 and U850 From January To June Initial Conditions

Initial Conditions	COR	RMSE	MSSS	SRATE (%)
		NATLSST + WPVZWS		
Jun	0.73	3.09	0.53	58
May	0.74	3.07	0.54	58
Apr	0.74	3.04	0.54	77
Mar	0.61	3.59	0.37	71
Feb	0.49	3.96	0.23	55
Jan	0.46	4.08	0.18	61
		NATLSST + U850		
Jun	0.66	3.40	0.43	55
May	0.72	3.15	0.51	61
Apr	0.68	3.30	0.46	71
Mar	0.58	3.70	0.33	71
Feb	0.50	3.95	0.23	55
Jan	0.45	4.12	0.16	58
		HGT500 + WPVZWS		
Jun	0.78	2.83	0.61	77
May	0.77	2.86	0.60	71
Apr	0.79	2.75	0.63	74
Mar	0.61	3.59	0.37	74
Feb	0.47	4.03	0.20	42
Jan	0.55	3.80	0.29	55
		HGT500 + U850		
Jun	0.73	3.11	0.52	74
May	0.77	2.90	0.59	77
Apr	0.77	2.89	0.59	77
Mar	0.59	3.65	0.34	74
Feb	0.49	3.95	0.23	52
Jan	0.56	3.77	0.30	58

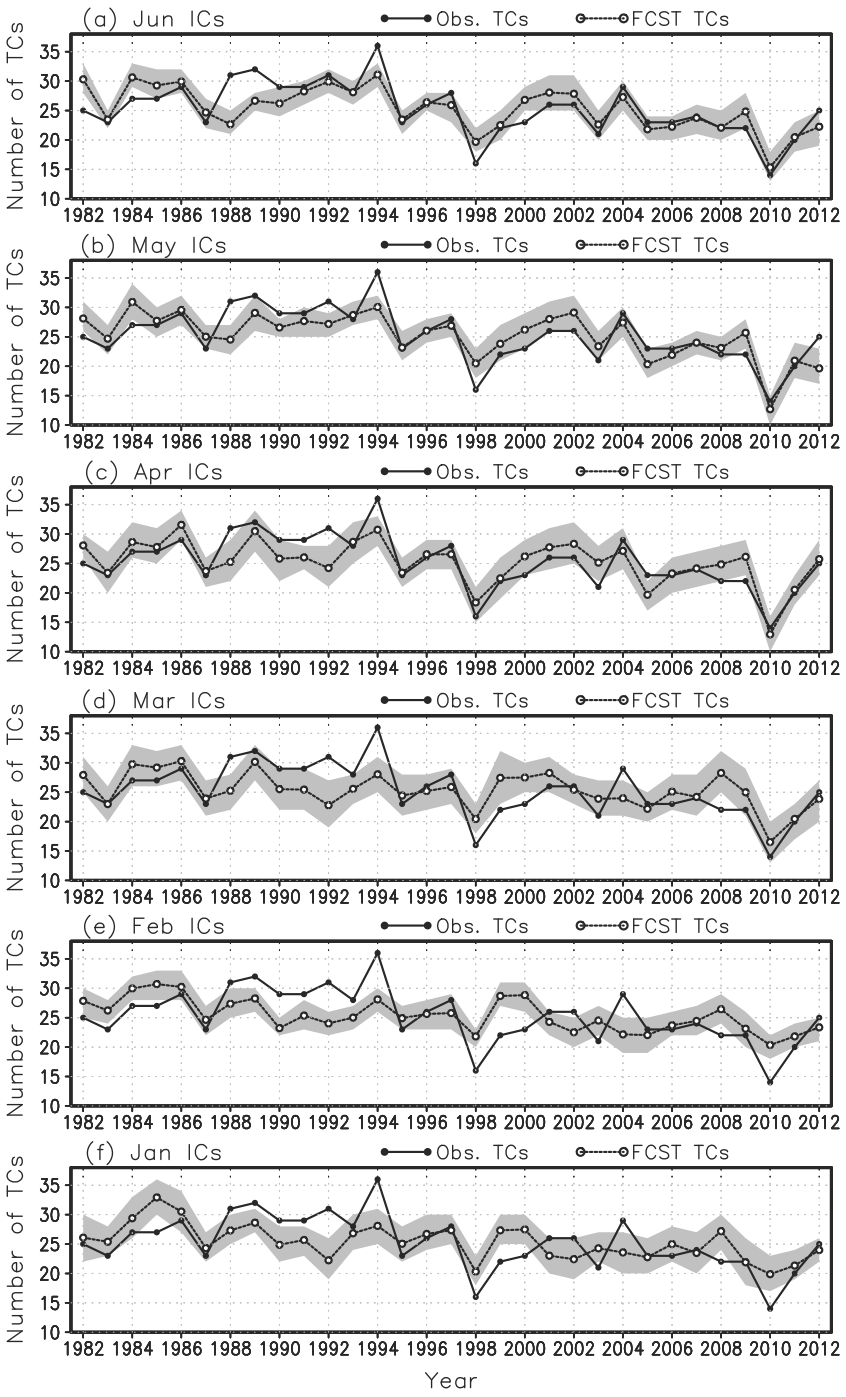

Figure 9. Time series of observed (black solid lines with closed circles) and hindcast (lines with open circles) ANTCs using the HGT500 + WPVZWS predictor model from 1982 to 2012 with (a) June, (b) May, (c) April, (d) March, (e) February, and (f) January initial conditions. Shadings indicate ±1 standard deviation of the spreads among 24 ensemble members.

[28] For the NATLSST and U850 combination, the hindcasts of WNP TC activity are shown in Table 4. At the 0–2 month leads, the correlations, RMSEs, MSSSs, and SRATEs range from 0.66 to 0.72, 3.15 to 3.40, 0.43 to 0.51, and 55% to 71%, respectively. For the longer leads, the hindcasts also exhibit relatively low skill.

[29] The hindcasts of WNP TC activity using HGT500 and WPVZWS as the predictors are shown in Table 4. The hindcasts provide the highest correlations ranging from 0.77 to 0.79, the lowest RMSEs ranging from 2.75 to 2.86, and the highest MSSSs ranging from 0.60 to 0.63, while the SRATEs are about 74% at 0–2 month leads. In contrast, at the 0–2 month leads, the HGT500 and U850 predictor model shows relatively low skill compared to the former combination, with correlations, RMSEs, MSSSs and SRATEs being around 0.75, 3.0, 0.56, and 76%, respectively (Tables 4). Both combinations show substantial low hindcast skills in the long leads.

Table 5. Forecast Model Using Two Predictors HGT500 and WPVZWS for El Niño Years and La Niña Years From January To June Initial Conditions

Initial Conditions	El Niño Years		La Niña Years		Neutral Years	
	RMSE	SRATE (%)	RMSE	SRATE (%)	RMSE	SRATE (%)
Jun	3.04	75	3.62	56	2.00	93
May	3.12	63	3.22	67	2.41	79
Apr	3.05	50	2.44	89	2.75	79
Mar	3.95	75	3.70	56	3.28	86
Feb	4.35	50	4.63	22	3.38	50
Jan	3.86	63	4.22	33	3.47	64

[30] Overall, the hybrid system with predictors HGT500 and WPVZWS combination has the greatest skill in the 31 year hindcast of ANTCs. However, it is noticed that the hindcasts at the 1 and 2 month leads with single predictor or combinations may have better performance compared to the 0 month lead hindcasts, including the HGT500 and WPVZWS model.

[31] Figure 9 presents the observed and hindcast ANTCs for 1982–2012 based on the HGT500 and WPVZWS predictor model with January to June ICs. The hindcast captures the five active years of 1986, 1990, 1991, 1992, and 2004 and the six inactive years of 1999, 2003, 2008, 2009, 2010, and 2011 but misses the active (inactive) years of 1988, 1989, and 1994 (1998) (Figure 9a). In contrast, the hindcasts capture 9 years of active and inactive seasons at 1–2 month leads (Figures 9b and 9c). As expected, the hindcasts show lower skills in capturing ANTC activity at 3–5 month leads (Figures 9d–9f). As mentioned above, we demonstrate that in spite of the slightly low performances of the model at 0 month lead, the model performs very well in capturing ANTC occurrences across most of the active and inactive years characterized by higher SRATEs. However, some extreme ANTC activity is not well predicted by the model at 0–2 month leads.

[32] In the following section, we examine the capability of the HGT500 and WPVZWS model in capturing the ANTC occurrence during ENSO events. We also explain why the model at 1–2 month leads performs slightly better in reaching the highest correlations, lowest RMSEs, and greatest MSSSs.

5.2. ENSO Years

[33] ENSO years are identified based on the Niño-3.4 index during the TC season. The El Niño years are 1982, 1987, 1991, 1994, 1997, 2002, 2004, and 2009; the La Niña years are 1984, 1985, 1988, 1995, 1998, 1999, 2000, 2007, and 2010; and the remaining years are neutral. The model performs well during the ENSO years (Table 5). At the 0–2 month leads, the hindcasts capture the ANTCs during El Niño years with RMSEs of 3.04, 3.12, and 3.05 and SRATEs of 75%, 63%, and 50%. They also capture the ANTCs during La Niña years, with RMSEs of 3.62, 3.22, and 2.44 and SRATEs of 56%, 67%, and 89%, respectively. It is notable that the forecast skills for La Niña years at 1–2 month leads are higher than the skill at 0 month lead, especially the skill at 2 month lead, with a RMSE of 2.44. During 89% of the La Niña years, ANTC hindcasts fall within one standard deviation of the 24-member spreads. As lead time increases from 3 months to 5 months, the HGT500 and WPVZWS model has less skill in capturing ANTCs during the ENSO years, with an increase in the RMSEs from 3.86 to 4.63.

[34] In general, as time lead increases, the model hindcasts skills in El Niño and neutral years decrease, except for La Niña years, suggesting that the higher RMSEs for 31 year hindcasts at the 0 month lead compared

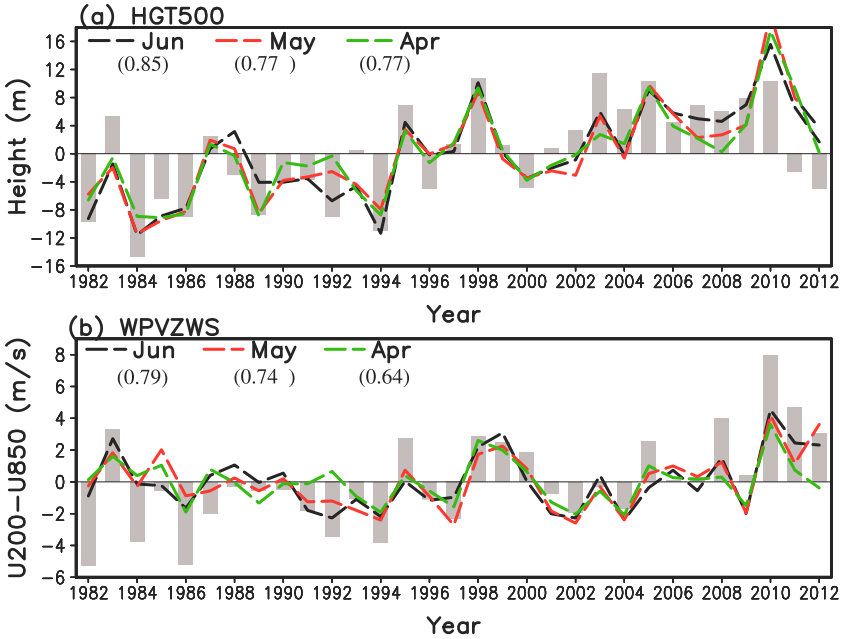

Figure 10. Temporal evolution of JASO area averaged anomaly for predictors (a) HGT500 and (b) WPVZWS from observations (gray bars) and CFSv2 24-member ensemble means with June (black solid lines), May (red solid lines), and April (green solid lines) initial conditions. Numbers indicate the mean correlation coefficient over 31 years.

Table 6. Forecasts of the Annual Western Pacific TCs Using HGT500 and WPVZWS Predictor Model and Other Forecast Models for the 2003–2012 TC Seasons[a]

		CFSv2			TSR			GCACIC	
Year	Obs	March ICs	May ICs	June ICs	March/April	May/June	Early July	April	June
2003	21	25(23–28)	23(21–25)	23(21–25)	26.7(±5.1)	25.8(±4.8)	26.3(±4.9)	26	26
2004	29	26(24–29)	28(26–30)	28(26–30)	25.9(±5.1)	26.6(±4.9)	27.0(±5.0)	29	29
2005	23	24(22–26)	19(17–21)	22(21–23)	25.9(±4.0)	27.6(±3.7)	27.6(±3.7)	24	25
2006	23	26(24–28)	21(19–23)	22(21–24)	27.1(±4.0)	29.0(±3.7)	29.0(±3.7)	27	28
2007	24	25(22–28)	24(22–26)	24(22–26)	24.3(±3.9)	26.8(±3.7)	26.8(±3.7)	25	24
2008	22	28(25–31)	22(20–24)	22(20–24)	28.3(±3.7)	28.3(±3.7)	28.3(±3.7)	30	30
2009	22	25(22–28)	26(24–29)	25(23–27)	25.6(±3.9)	27.5(±3.8)	28.0(±3.9)	27	27
2010	14	16(14–18)	11(9–14)	15(13–17)	24.2(±3.8)	24.1(±3.8)	23.0(±3.8)	24	23
2011	20	20(18–23)	21(19–23)	20(19–22)	27.8(±4.2)	28.0(±4.0)	28.3(±4.0)	27	27
2012	25	24(21–27)	20(18–23)	22(20–25)	25.5(±4.6)	25.5(±4.6)	26.8(±4.2)	N/A	N/A
RMSE		3.08	2.74	1.55	5.34	5.74	5.71	5.59	5.51
SRATE(%)		70	70	90					
2013		23(21–26)	21(20–22)	22(20–24)		25.5(±4.2)	25.4(±4.3)		

[a]Values in parentheses are the possible range of annual western Pacific TC forecasts. The observed annual number of TCs (Obs), RMSE, and SRATE of the forecasts over 10 years are presented. Forecasts for the 2013 season based on the CFSv2 predictions and issued by TSR are also listed.

to those at the 1–2 month leads are resulted from the relatively poor performance of the CFSv2 system in predicting ENSO-related climate variability at the 0 month lead. The failure in capturing the ANTC variability at the 0 month lead could be mainly resulted from the contributions of a number of years: 1988, 1989, and 1998, the strong ENSO-related events (Figure 9a).

[35] *Jin et al*. [2008] and *Kim et al*. [2011] have compared the seasonal prediction skills for ENSO in various dynamical models. They suggested that the growing phases of ENSO events were better predicted than the corresponding decaying phases. In the springs of 1988 and 1998, the 1987 and 1997 El Niño episodes were in a decaying phase, followed immediately by strong La Niña events. The decaying phase of La Niña in 1988 was found from October 1988 to July 1989, while the La Niña condition in 1998 remained a cold episode throughout 1999 and into the year 2000. Figure 10 presents the year-to-year variability of JASO area-averaged anomalies for predictors HGT500 and WPVZWS at the 0–2 month leads. In spite of the highest correlations between observation and CFSv2 predictions at the 0 month lead, the CFSv2 prediction at the 1 month or 2 month lead shows slightly good skills in 1988, 1989, and 1998 when ENSO episodes were in decaying phase and rapid transitions, consistent with previous findings [*Jin et al*., 2008; *Kim et al*., 2011].

5.3. Comparing With Other Models

[36] To summarize, the forecast skills of the two-predictor models using CFSv2 0–2 month leads predictions are higher than those using 3–5 month leads. The HGT500 and WPVZWS model has the greatest skill in the 31 year hindcast of ANTCs among all two-predictor models. This combination is thus selected in the final configuration of the empirical prediction model.

[37] The dynamical-statistical forecast model developed in this study is evaluated further by comparing it with previous operational statistical forecasts issued by the Tropical Storm Risk (referred to as TSR, http://www.tropicalstormrisk.com) and the Guy Carpenter Asia-Pacific Climate Impact Centre (referred to as GCACIC [*Chan et al*., 2001], http://www.cityu.edu.hk/gcacic/pacific.htm) for the past 10 years (2003–2012). These models are purely statistical models which are based on lagged relationships between TC activity and preseason atmosphere/ocean conditions in observations. For this comparison, the data used in the regression analysis consist of only years prior to the target year. To make a forecast for 2003, for example, we use the CFSv2-predicted JASO HGT500 and WPVZWS for 1982–2002 to establish the relationship with the observed ANTC activity using the multiple linear regression technique.

[38] Table 6 lists the forecasts of ANTCs for the 2003–2012 seasons with the CFSv2-predicted JASO HGT500 and WPVZWS at 3 month (March ICs), 1 month (May ICs), and 0 month (June ICs) leads and those issued by the TSR and GCACIC during March to early July. The actual number of annual WNP TCs in each year, RMSE, SRATE, and the possible range of the forecasts are also listed in Table 6. Given a forecasted value based on ensemble mean predictors and a standard deviation of individual member forecast spreads, the possible range of TC numbers can be determined. The forecasts based on the regression equations are rounded to the nearest integer to obtain the number of TCs. The result suggests that the annual TC forecast based on the CFSv2-predicted large-scale geopotential height and vertical zonal wind shear is competitive with the TSR and GCACIC forecast schemes. The CFSv2 forecasts at 0–1 month leads have smaller RMSE than those at 3 month lead. The SRATEs at 3 and 1 month leads are up to 70% with only 3 years (30%) out of a total of 10 being outside of the model standard deviation. At the 0 month lead, the observed ANTC totals are captured within the forecast range in 9 of 10 inactive years (except 2009), displaying that the hindcasts based on the CFSv2 predictions at 0 month lead are more skillful. The ANTCs in 2013 season forecasts yielded from the hybrid system, as well as the forecast range, are also listed in Table 6, showing that the season is an inactive season.

6. Concluding Remarks

[39] This study presents a substantial improvement in the potential for more accurate statistical forecasting of the annual TC activity over the western North Pacific by using a hybrid dynamical-statistical model. The prediction model is built upon the empirical relationships between the interannual

variability of the actual annual number of TCs (ANTCs) and the variability of large-scale atmospheric and oceanic variables in the CFSv2 seasonal mean hindcasts for JASO.

[40] The approach comprises an identification of potentially skillful predictors during JASO that represent important main metrics for predicting the annual TC formation. They are (1) the tropical North Atlantic SST (NATLSST), which exerts a remote influence on the anomalous anticyclone over the central Pacific and WNP that is unfavorable for TC formation; (2) vertical zonal wind shear between 200 hPa and 850 hPa over the tropical WNP (WPVZWS); and (3) the zonal wind at 850 hPa over the tropical WNP (U850). The positive anomalies of U850 indicate that an eastward extension of the monsoon trough coincides with reduced WPVZWS, implying a favorable large-scale environmental factor for TC formation. The predictors also include (4) the 500 hPa geopotential height over the subtropical WNP (HGT500) where colder middle-lower troposphere air masses support the development of TCs. Then, the four predictors (Table 1) derived from the CFSv2 24-member ensemble forecasts for JASO are incorporated into a linear regression model to predict the WNP TC totals.

[41] Using the hybrid model with the four potential predictors singularly or in combination, we assess the WNP TC hindcast skill for 1982–2012 through leave-one-out cross validation. Four 2-predictor combinations except one 2-predictor model with NATLSST and U850 are more skillful than one-predictor HGT500 model by the assessment of correlation coefficients and the root-mean-square errors (RMSEs) between observed and hindcast ANTCs (Tables 2 and 4). The forecasts based on NATLSST and WPVZWS, and on NATLSST and U850, from the CFSv2 predictions have a similar skill, producing correlations higher than 0.70 and around 70% interannual variations of WNP TCs within the hindcast boundaries of standard deviation (SRATE) at shorter leads. In contrast, using the combination of HGT500 and WPVZWS, and HGT500 and U850, the hindcasts achieve a greater skill with correlations, RMSEs, and SRATEs ranging from 0.73 to 0.79, 3.11 to 2.75, and 71% to 77%, respectively.

[42] Using the most skillful combination of HGT500 and WPVZWS, the hybrid system demonstrates generally well the performances during El Niño years, with RMSEs slightly high than those of 31 year hindcasts (Table 5). The relatively poor performances of dynamic model predictions in capturing the ENSO events in decaying phases and the rapid transition from El Niño to La Niña conditions [*Jin et al*., 2008; *Kim et al*., 2011] could be the main cause for small skill in capturing the ANTCs during La Niña years at short leads, rather than a deficiency of regression in the model.

[43] Furthermore, for the past 10 years from 2003 to 2012, in comparison to the current forecast schemes in operations, the HGT500 and WPVZWS model achieves RMSEs and SRATEs ranging from 3.08 to 1.55 and from 70% to 90% with March to June ICs, respectively (Table 6). The result shows that the hybrid system is quite compelling. The forecasts for ANTCs in the 2013 season yielded from the hybrid system show that the season is an inactive season.

[44] **Acknowledgments.** We thank Wanqiu Wang for providing the CFSv2 real-time forecasts. We also thank Zeng-Zhen Hu and three anonymous reviewers for constructive comments and suggestions. This research was partially supported by the National Natural Science Foundation of China grant 41365005, the National Technology Research and Development Program grant 2013BAK05B03, the Meteorological Public Welfare Scientific Research Project grant GYHY201106010, and the Sun Yat-sen University "985 Project" Phase 3. The manuscript was prepared while the first author was a visiting scientist at the NOAA Climate Prediction Center.

References

Ashok, K., S. K. Behera, S. A. Rao, H. Weng, and T. Yamagata (2007), El Niño Modoki and its possible teleconnection, *J. Geophys. Res.*, *112*, C11007, doi:10.1029/2006JC003798.

Camargo, S. J., and A. H. Sobel (2005), Western North Pacific tropical cyclone intensity and ENSO, *J. Clim.*, *18*, 2996–3006, doi:10.1175/JCLI3457.1.

Camargo, S. J., K. A. Emanuel, and A. H. Sobel (2007a), Use of a genesis potential index to diagnose ENSO effects on tropical cyclone genesis, *J. Clim.*, *20*, 4819–4834, doi:10.1175/JCLI4282.1.

Camargo, S. J., A. W. Robertson, S. J. Gaffney, P. Smyth, and M. Ghil (2007b), Cluster analysis of typhoon tracks. Part II: Large-scale circulation and ENSO, *J. Clim.*, *20*, 3654–3676, doi:10.1175/JCLI4203.1.

Chan, J. C. L. (1995), Tropical cyclone activity in the western North Pacific in relation to the stratospheric quasi-biennial oscillation, *Mon. Weather Rev.*, *123*, 2567–2571, doi:10.1175/1520-0493(1995)123<2567:TCAITW>2.0.CO;2.

Chan, J. C. L. (2000), Tropical cyclone activity over the western North Pacific associated with El Niño and La Niña events, *J. Clim.*, *13*, 2960–2972, doi:10.1175/1520-0442(2000)013<2960:TCAOTW>2.0.CO;2.

Chan, J. C. L. (2007), Interannual variations of intense typhoon activity, *Tellus, Ser. A*, *59*, 455–460, doi:10.1111/j.1600-0870.2007.00241.x.

Chan, J. C. L. (2008), A simple seasonal forecast update of tropical cyclone activity, *Weather Forecast.*, *23*, 1016–1021, doi:10.1175/2008WAF2007061.1.

Chan, J. C. L., and K. S. Liu (2004), Global warming and western North Pacific typhoon activity from an observational perspective, *J. Clim.*, *17*, 4590–4602, doi:10.1175/3240.1.

Chan, J. C. L., J.-E. Shi, and C. M. Lam (1998), Seasonal forecasting of tropical cyclone activity over the western North Pacific and the South China Sea, *Weather Forecast.*, *13*, 997–1004, doi:10.1175/1520-0434(1998)013<0997:SFOTCA>2.0.CO;2.

Chan, J. C. L., J.-E. Shi, and K. S. Liu (2001), Improvements in the seasonal forecasting of tropical cyclone activity over the western North Pacific, *Weather Forecast.*, *16*, 491–498, doi:10.1175/1520-0434(2001)016<0491:IITSFO>2.0.CO;2.

Chang, P., L. Ji, and H. Li (1997), A decadal climate variation in the tropical Atlantic Ocean from thermodynamic air-sea interactions, *Nature*, *385*, 516–518, doi:10.1038/385516a0.

Chen, J.-H., and S.-J. Lin (2011), The remarkable predictability of inter-annual variability of Atlantic hurricanes during the past decade. *Geophys. Res. Lett.*, *38*, L11804, doi:10.1029/2011GL047629.

Chen, J.-H., and S.-J. Lin (2013), Seasonal predictions of tropical cyclones using a 25-km resolution general circulation model, *J. Clim.*, *26*, 380–298.

Chen, T.-C., S.-P. Weng, N. Yamazaki, and S. Kiehne (1998), Interannual variation in the tropical cyclone formation over the western North Pacific, *Mon. Weather Rev.*, *126*, 1080–1090, doi:10.1175/1520-0493(1998)126<1080:IVITTC>2.0.CO;2.

Chu, P.-S., and X. Zhao (2007), A Bayesian regression approach for predicting seasonal tropical cyclone activity over the central North Pacific, *J. Clim.*, *20*, 4002–4012, doi:10.1175/JCLI4214.1.

Elsner, J. B., and C. P. Schmertmann (1993), Improving extended-range seasonal predictions of intense Atlantic hurricane activity, *Weather Forecast.*, *8*, 345–351, doi:10.1175/1520-0434(1993)008<0345:IERSPO>2.0.CO;2.

Enfield, D. B., and D. A. Mayer (1997), Tropical Atlantic sea surface temperature variability and its relation to El Niño–Southern Oscillation, *J. Geophys. Res.*, *102*, 929–945, doi:10.1029/96JC03296.

Fan, K. (2007a), North Pacific sea ice cover, a predictor for the western North Pacific typhoon frequency?, *Sci. China, Ser. D Earth Sci.*, *50*, 1251–1257, doi:10.1007/s11430-007-0076-y.

Fan, K. (2007b), New predictors and a new prediction model for the typhoon frequency over western North Pacific, *Sci. China. Ser. D Earth Sci.*, *50*, 1417–1423, doi:10.1007/s11430-007-0105-x.

Fan, K., and H. Wang (2009), A new approach to forecasting typhoon frequency over the western North Pacific, *Weather Forecast.*, *24*, 974–986, doi:10.1175/2009WAF2222194.1.

Gray, W. M. (1984a), Atlantic seasonal hurricane frequency. Part I: El Niño and 30-mb quasi-biennial oscillation influences, *Mon. Weather Rev.*, *112*, 1649–1668, doi:10.1175/1520-0493(1984)112<1649:ASHFPI>2.0.CO;2.

Gray, W. M. (1984b), Atlantic seasonal hurricane frequency. Part II: Forecasting its variability, *Mon. Weather Rev.*, *112*, 1669–1683, doi:10.1175/1520-0493(1984)112<1669:ASHFPI>2.0.CO;2.

Gray, W. M., C. W. Landsea, P. W. Mielke, and K. J. Berry (1993), Predicting Atlantic basin seasonal hurricane activity by 1 August, *Weather Forecast.*, *8*, 73–86, doi:10.1175/1520-0434(1993)008<0073:PABSTC>2.0.CO;2.

Gray, W. M., C. W. Landsea, P. W. Mielke, and K. J. Berry (1994), Predicting Atlantic basin seasonal hurricane activity by 1 June, *Weather Forecast.*, *9*, 103–115, doi:10.1175/1520-0434(1994)009<0103:PABSTC>2.0.CO;2.

Ho, C.-H., and H.-S. Kim, J.-H. Jeong, and S.-W. Son (2009), Influence of stratospheric quasi-biennial oscillation on tropical cyclone tracks in the western North Pacific, *Geophys. Res. Lett.*, *36*, L06702, doi:10.1029/2009GL037163.

Hu, Z.-Z., A. Kumar, B. Huang, Y. Xue, W. Wang, and B. Jha (2011), Persistent atmospheric and oceanic anomalies in the North Atlantic from summer 2009 to summer 2010, *J. Clim.*, *24*, 5812–5830, doi:10.1175/2011JCLI4213.1.

Hu Z.-Z., A. Kumar, B. Huang, W. Wang, J. Zhu, and C. Wen (2012), Prediction skill of monthly SST in the North Atlantic Ocean in NCEP Climate Forecast System version 2, *Clim. Dyn.*, doi:10.1007/s00382-012-1431-z, published online.

Huang, B., P. S. Schopf, and Z. Pan (2002), The ENSO effect on the tropical Atlantic variability: A regionally coupled model study, *Geophys. Res. Lett.*, *29*(21), 2039, doi:10.1029/2002GL014872.

Jia, X., and S. Yang (2013), Impacts of the quasi-biweekly oscillation over the western North Pacific on East Asian subtropical monsoon during early summer, *J. Geophys. Res. Atmos*, *118*, 1–14, doi:10.1002/jgrd.50422.

Jiang, X., S. Yang, Y. Li, A. Kumar, X. Liu, Z. Zuo, and B. Jha (2013a), Seasonal-to-interannual prediction of the Asian summer monsoon in the NCEP Climate Forecast System version 2, *J. Clim.*, *26*, 3708–3727, doi:10.1175/JCLI-D-12-00437.1.

Jiang, X., S. Yang, Y. Li, A. Kumar, W. Wang, and Z. Gao (2013b), Dynamical prediction of the East Asian winter monsoon by the NCEP Climate Forecast System, *J. Geophys. Res. Atmos*, *118*, 1312–1328, doi:10.1002/jgrd.50193.

Jin, E. K., et al. (2008), Current status of ENSO prediction skill in coupled ocean-atmosphere models, *Clim. Dyn.*, *31*, 647–664, doi:10.1007/s00382-008-0397-3.

Kim, H.-M., and P. J. Webster (2010), Extended-range seasonal hurricane forecasts for the North Atlantic with a hybrid dynamical-statistical model, *Geophys. Res. Lett.*, *37*, L21705, doi:10.1029/2010GL044792.

Kim, J.-H., C.-H. Ho, and P.-S. Chu (2010), Dipolar redistribution of summertime tropical cyclone genesis between the Philippine Sea and the northern South China Sea and its possible mechanism, *J. Geophys. Res.*, *115*, D06104, doi:10.1029/2009JD012196.

Kim, H.-M., P. J. Webster, and J. A. Curry (2011), Modulation of North Pacific tropical cyclone activity by three phases of ENSO, *J. Clim.*, *24*, 1839–1849, doi:10.1175/2010JCLI3939.1.

Kim, H.-M., P. J. Webster, and J. A. Curry (2012a), Seasonal prediction skill of ECMWF System 4 and NCEP CFSv2 retrospective forecast for the Northern Hemisphere winter, *Clim. Dyn.*, *39*, 2957–2973, doi:10.1007/s00382-012-1364-6.

Kim, H.-M., P. J. Webster, J. A. Curry, and V. E. Toma (2012b), Asian summer monsoon prediction in ECMWF System 4 and NCEP CFSv2 retrospective seasonal forecasts, *Clim. Dyn.*, *39*, 2975–2991, doi:10.1007/s00382-012-1470-5.

Kim, H.-S., C.-H. Ho, J.-H. Kim, and P.-S. Chu (2012), Track-pattern-based model for seasonal prediction of tropical cyclone activity in the western North Pacific, *J. Clim.*, *25*, 4660–4678, doi:10.1175/JCLI-D-11-00236.1.

Klotzbach, P. J., and W. M. Gray (2004), Updated 6–11 month prediction of Atlantic basin seasonal hurricane activity, *Weather Forecast.*, *19*, 917–934, doi:10.1175/1520-0434(2004)019<0917:UMPOAB>2.0.CO;2.

Liu, Z., Q. Zhang, and L. Wu (2004), Remote impact on tropical Atlantic climate variability: Statistical assessment and dynamic assessment, *J. Clim.*, *17*, 1529–1549, doi:10.1175/1520-0442(2004)017<1529:RIOTAC>2.0.CO;2.

Liu, X., S. Yang, A. Kumar, S. Weaver, and X. Jiang (2013), Diagnostics of sub-seasonal prediction biases of the Asian summer monsoon by the NCEP Climate Forecast System, *Clim. Dyn.*, *41*, 1453–1474.

Lu, R., and B. Dong (2005), Impact of Atlantic sea surface temperature anomalies on the summer climate in the western North Pacific during 1997–1998, *J. Geophys. Res.*, *110*, D16102, doi:10.1029/2004JD005676.

Reynolds, R. W., N. A. Rayner, T. M. Smith, D. C. Stokes, and W. Wang (2002), An improved in situ and satellite SST analysis for climate, *J. Clim.*, *15*, 1609–1625, doi:10.1175/1520-0442(2002)015<1609:AIISAS>2.0.CO;2.

Richard, C., Y. Li, and W. Zhou (2012), Changes in western Pacific tropical cyclones associated with the El Niño–Southern Oscillation cycle, *J. Clim.*, *25*, 5864–5878, doi:10.1175/JCLI-D-11-00430.1.

Rong, X. Y., R. H. Zhang, and T. Li (2010), Impacts of Atlantic sea surface temperature anomalies on Indo-East Asian summer monsoon-ENSO relationship, *Chinese Science Bull.*, *55*, 2458–2468, doi:10.1007/s11434-010-3098-3.

Saha, S., et al. (2010), The NCEP Climate Forecast System reanalysis, *Bull. Am. Meteorol. Soc.*, *91*, 1015–1057, doi:10.1175/2010BAMS3001.1.

Sun, J. Q., and H. P. Chen (2011), Predictability of western North Pacific typhoon activity and its factors using DEMETER coupled models, *Chin. Sci. Bull.*, *56*, 3474–3479, doi:10.1007/s11434-011-4640-7.

Vecchi, G. A., M. Zhao, H. Wang, G. Villarini, A. Rosati, A. Kumar, I. M. Held, and R. Gudgel (2011), Statistical-dynamical predictions of seasonal North Atlantic hurricane activity, *Mon. Weather Rev.*, *139*, 1070–1082, doi:10.1175/2010MWR3499.1.

Vitart, F. (2006), Seasonal forecasting of tropical storm frequency using a multi-model ensemble, *Q. J. R. Meteorol. Soc.*, *132*, 647–666, doi:10.1256/qj.05.65.

Vitart, F., M. Huddleston, M. Deque, D. Peake, T. Palmer, T. Stockdale, M. Davey, S. Ineson, and A. Weisheimer (2007), Dynamically-based seasonal forecast of Atlantic tropical storm activity issued in June by EUROSIP, *Geophys. Res. Lett.*, *34*, L16815, doi:10.1029/2007GL030740.

Wang, B., and J. C. L. Chan (2002), How strong ENSO events affect tropical storm activity over the western North Pacific, *J. Clim.*, *15*, 1643–1658, doi:10.1175/1520-0442(2002)015<1643:HSEEAT>2.0.CO;2.

Wang, H. J., and K. Fan (2007), Relationship between the Antarctic oscillation and the western North Pacific typhoon frequency, *Chin. Sci. Bull.*, *52*, 561–565, doi:10.1007/s11434-007-0040-4.

Wang, H. J., J. Q. Sun, and K. Fan (2007), Relationships between the North Pacific Oscillation and typhoon and hurricane frequencies, *Sci. China. Ser. D Earth Sci.*, *50*, 1409–1416, doi:10.1007/s11430-007-0097-6.

Wang, H., J.-K. Schemm, A. Kumar, W. Wang, L. Long, M. Chelliah, G. D. Bell, and P. Peng (2009), A statistical forecast model for Atlantic seasonal hurricane activity based on the NCEP dynamical seasonal forecast, *J. Clim.*, *22*, 4481–4500, doi:10.1175/2009JCLI2753.1.

Wang, W., P. Xie, S. H. Yoo, Y. Xue, A. Kumar, and X. Wu (2011), An assessment of the surface climate in the NCEP Climate Forecast System Reanalysis, *Clim. Dyn.*, *37*, 1601–1620, doi:10.1007/s00382-010-0935-7.

Werner, A., and N. J. Holbrook (2011), A Bayesian forecast model of Australian region tropical cyclone formation, *J. Clim.*, *24*, 6114–6131, doi:10.1175/2011JCLI4231.1.

Wilks, D. S. (2006), *Statistical Methods in the Atmospheric Science*, 2nd ed., pp. 627, Elsevier.

Wu, L., Z. Wen, R. Huang, and R. Wu (2012), Possible linkage between the monsoon trough variability and the tropical cyclone activity over the western North Pacific, *Mon. Weather Rev.*, *140*, 140–150, doi:10.1175/MWR-D-11-00078.1.

Xue, Y., B. Huang, Z. Z. Hu, A. Kumar, C. Wen, and D. Behringer (2011), An assessment of oceanic variability in the NCEP climate forecast system reanalysis, *Clim. Dyn.*, *37*, 2511–2539, doi:10.1007/s00382-010-0954-4.

Zhan, R. F., Y. Wang, and X. Lei (2011), Contributions of ENSO and East Indian Ocean SSTA to the interannual variability of Northwest Pacific tropical cyclone frequency, *J. Clim.*, *24*, 509–521, doi:10.1175/2010JCLI3808.1.

Zhao, M., I. M. Held, and G. A. Vecchi (2010), Retrospective forecast of the hurricane season using a global atmospheric model assuming persistence of SST anomalies, *Mon. Weather Rev.*, *138*, 3858–3868, doi:10.1175/2010MWR3366.1.

Zhao, H., L. Wu, and W. Zhou (2011), Interannual changes of tropical cyclone intensity in the western North Pacific, *J. Meteor. Soc. Japan*, *89*, 243–253, doi:10.2151/jmsj.2011-305.

Zhou, B. T., and X. Cui (2008), Hadley circulation signal in the tropical cyclone frequency over the western North Pacific, *J. Geophys. Res.*, *113*, D16107, doi:10.1029/2007JD009156.

Zhou, B. T., and X. Cui (2011), Sea surface temperature east of Australia: A predictor of tropical cyclone frequency over the western North Pacific?, *Chin. Sci. Bull.*, *56*, 196–201, doi:10.1007/s11434-010-4157-5.